The following publication Z. Qin et al., "A GPU-Based Grid Traverse Algorithm for Accelerating Lightning Geolocation Process," in IEEE Transactions on Electromagnetic Compatibility, vol. 62, no. 2, pp. 489-497, April 2020 is available at https://doi.org/10.1109/TEMC.2019.2907715.

A GPU-Based Grid Traverse Algorithm for Accelerating Lightning Geolocation Process

Zilong Qin, *Member*, *IEEE*, Mingli Chen, Fanchao Lyu, *Member*, *IEEE*,

Steven A. Cummer, *Fellow*, *IEEE*, Baoyou Zhu, Feifan Liu, Yaping Du

***Abstract*—Most lightning location networks are based on real-time analytical solutions of certain simplified models, while the reality is much more complicated. In this paper, we introduce a GPU-based parallel computing algorithm that can extensively benefit lightning geolocation networks. For a network running this GPU-based algorithm, one can build up a geolocation database based on numerical solutions of certain complete models in advance, lightning geolocations can then be easily determined with a grid searching technique in real-time. One such a grid searching technique is the grid traverse algorithm (GTA) for the traditional time of arrival (TOA) technique. By running GPU-based GTA in a 6-station-2D and a 5-station 3D networks, we show that extremely high network performance can be achieved, with a processing speed of about 2700 times faster than CPU-based GTA. The location accuracy of GPU-GTA is examined with Monte Carol simulations, showing that GPU-GTA can locate a lightning source in real time with high accuracy. We also find that when the grid step is comparable with the inherent time uncertainty of a network, the location accuracy cannot be improved further with a finer grid step.**

***Index Terms*—GPU-based computing algorithm, lightning electromagnetic pulse, lightning source location, time of arrival technique.**

I. Introduction

Lightning locations from ground-based lightning location networks provide fundamental information for scientific researches as well as the society of meteorology. Either in a long baseline 2-Dimensional (2D) lightning location network [1-16] or a 3-Dimensional (3D) Lightning Mapping Array (LMA) [17-28], the geolocation algorithm is always a critical technique to operate the network. Generally, there are three basic lightning geolocation techniques or their combinations that were deployed in existing networks. They are the Time of Arrival (TOA) technique [29], the Magnetic Direction Finder (MDF) technique [30] and the interferometric direction-finding technique, as well as their combination [31]. In a long baseline lightning location network operating essentially in ELF/VLF bands, the Time of Group Arrival (TOGA) technique is preferred [5, 32]. The interferometric direction-finding technique is widely used in 2D short baseline VHF interferometry systems [33-43]. The TOA technique is the basic method for most of the 3D lightning mapping arrays operating either in VHF or LF bands [17-25], while the interferometric direction-finding technique is also adopted in many 3D lightning mapping arrays [26-28]. The TOA technique finds the source location by matching the signal arrival time differences for each pair of sensors. For every two sensors (forming a baseline), the solution satisfying the TOAs to these two sensors will form a parabolic curve. By adding another proper baseline (another sensor), the source location that matches the arrival time differences of all baselines is the intersection point of the two parabolic curves. If the baselines are much shorter than the distances to the lightning source, finding the intersection point of the two parabolic curves becomes finding the direction of the line coinciding the two parabolic curves, which is the interferometric direction-finding technique. The TOGA technique estimates the lightning source distance by measuring the group delays of frequencies of lightning sferics above the cut-off frequency of the Earth-Ionosphere Waveguide (EIWG). The MDF technique identifies the source location by deploying the intersection of at least two azimuthal lines, each of which can be retrieved by orthogonal magnetic field measurements.

The lightning location based on the TOA technique can be solved with Chan's algorithm without iteration if the Earth curvature is ignorable. When the Earth curvature has to be considered, it turns to a non-linear optimization problem. The conventional method to tackle this kind of non-linear problem is to use the gradient search technique (e,g. Levenberg-Marquart and Newton-Raphson methods) [9, 29], which the initial value of the search is often estimated from Chan's algorithm with no consideration of the Earth curvature. Besides, there are also some TOA networks that adopt the CPU-based numerical grid traverse algorithm (GTA). Differing with the iteration algorithm, the GTA builds a grid database first, and then find the grid point that matches the time differences [17, 44]. Though computing burdensome, the GTA has some

Manuscript received xx; revised xx; accepted xx. This work was supported in part by Research Grant Council of Hong Kong Government under Grant PolyU152652/16E. (*Corresponding author: Mingli Chen*)

Z. Qin, M. Chen, F. Lyu and Y. Du are with Department of Building Service Engineering, The Hong Kong Polytechnic University, Hong Kong, China (e-mail: zilong.qin@connect.polyu.hk; mingli.chen@polyu.edu.hk; fanchao.lyu@gmail.com; ya-ping.du@polyu.edu.hk).

S. A. Cummer are with Electrical and Computer Engineering Department, Duke University, Durham, NC, USA (e-mail: cummer@duke.edu).

B. Zhu and F. Liu are with CAS Key Laboratory of Geospace Environment, School of Earth and Space Sciences, University of Science and Technology of China, Hefei, China (e-mail: zhuby@ustc.edu.cn; lff@mail.ustc.edu.cn).

advantages. It is much simpler than the iteration method, which does not need an initial value and is inherently accurate. Specifically, for radio geolocation applications, delays of radio wave propagation due to the Earth topography can be considered in GTA to improve the geolocation accuracy. The Earth topography has significant influences on the propagation of lightning electromagnetic waves, inducing the time uncertainty of TOA. In some networks, very sophisticated approaches for corrections of the sensor's site errors and the lightning field propagation time delays were adopted [45, 46]. Through quantitative estimation with FDTD wave modeling [47-49], time corrections for a given network can be obtained and easily input to the GTA database in advance, which can significantly improve the accuracy of the location network.

The CPU-based GTA algorithm usually has poor efficiency when extensive computing is needed, which limits its applications in real-time geolocation networks. With the development of Graphics Processing Unit (GPU) parallel computing technique, numerical computations can be largely accelerated [50]. In this study, we propose a GPU-based GTA algorithm, which is simple for implementation, and more efficient than a CPU-based GTA algorithm. Its applications to a 2D long-baseline network and a 3D short-baseline network show that GPU-GTA can work efficiently and accurately in locating a lightning source in either 2D or 3D. The high performance of GPU-GTA makes it a practical algorithm for accurately locating a lightning source in real-time.

II. TOA Lightning Location And GPU-based Parallel Computing Technique

TOA algorithm determines the geolocation of lightning sources with the difference of time of arrival of electromagnetic field signals from the same source to different sensors. It has been widely applied to both 2D [3] or 3D [19] lightning networks. Theoretically, TOA geolocation networks need at least 4 sensors to obtain 2D locations of the sources (latitude and longitude) and 5 sensors for 3D locations (latitude, longitude, and altitude). Some redundant sensors are required to get more reliable source locations. For one baseline containing 2 sensors, the arrival time difference can be written as:

$$\Delta t = t_2 - t_1 \qquad (1)$$

Where, t_1 and t_2 are the arrival times of the source waves measured at different sensors. Δt is the time difference between each two sensors, which can be measured taking the signal onset times, the windowed cross-correlation in broadband systems, or the phase difference in narrowband systems.

With multiple baselines, the solution of geolocation can be obtained by optimizing the objective function $f(\boldsymbol{r})$ as:

$$f(\boldsymbol{r}) = \sum_{i=1}^{N-1} |\Delta t_i - (\Delta t_i'(\boldsymbol{r}) + (\sigma_2 - \sigma_1))| \qquad (2)$$

Where N is the number of sensors, $\sigma_{1,2}$ the inherent propagation factors through each path, which can be pre-determined by the wave propagation modeling. $\Delta t_i'$ is the propagation time difference from a source location $\boldsymbol{r}$ to each sensor: $\Delta t_i'(\boldsymbol{r}) = \big(d(\boldsymbol{r}, \boldsymbol{r_i}) - d(\boldsymbol{r}, \boldsymbol{r_0})\big)/c$, where c is the speed of light and $d(\boldsymbol{r}, \boldsymbol{r_i})$ the distance along the propagating path. For a short-baseline network around 5-50 km, $d(\boldsymbol{r}, \boldsymbol{r_i})$ is usually defined as the straight distance between the source and the sensor [17-25]. For a short-baseline network like the Vaisala system, electromagnetic field signals from lightning emission sources propagate along the Earth surface, therefore, $d(\boldsymbol{r}, \boldsymbol{r_i})$ is defined as the spherical distance between the source and the sensor [1-4, 6-16]. For long-baseline network (above 3000 km) which essentially uses the ELF and VLF bands, the equation (2) is only suitable to signals with frequencies below the EIWG cut-off frequency (usually below 2 kHz, differs during day and nighttime). For frequencies which above the EIWG cut-off frequency, the TOGA method taking acount of the effects of the dispersion of the EIWG on the lightning sferics is much more preferred [32].While the conventional method solves the non-linear iteration Eq. (2) directly (the 3D iteration solver of Eq. (2) can be found in [29]) to find a solution, the grid traverse algorithm (GTA) traverses pre-built, discretized grids of the network region to find the best-fitted solution that has the smallest $f(\boldsymbol{r})$. It is straightforward but computing costly, and thus its overall performance, such as the speed and locating precision, relies heavily upon the grid step and the network coverage.

A sketch map of a pre-build discretized 2D region is shown in **Fig.1**. As illustrated in the figure, by computing $f(\boldsymbol{r})$ at each grid, the best-fitted source location can be retrieved by finding the grid having the smallest $f(\boldsymbol{r})$.

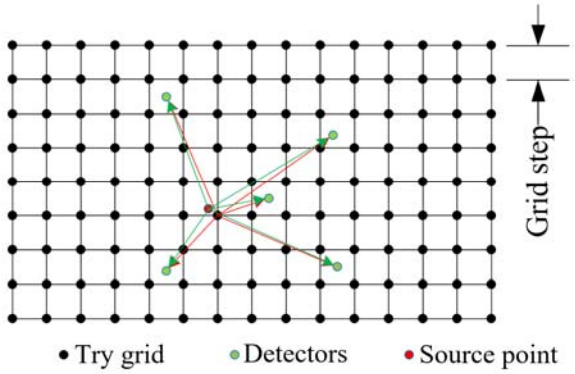

Fig.1 A sketch map of GTA in a lightning location network. Where the detection region is separated evenly in grid. Gary point is the location of a lightning source; blue points are the locations of sensors. Black points are the try locations in each grid.

A. *Traditional GTA with/without parallel computing*

The traditional GTA (CPU-GTA) calculates the $f(\boldsymbol{r})$ at each point, comparing them one by one and remaining the point that has the smaller $f(\boldsymbol{r})$, with the whole process being entirely in a serial way. The performance is rather poor when the detection region is large, and the grid step is small. Considering a 2D location situation, when the region is 1000 km South-North, and 1000 km East-West and the grid step is 250 m, a total of 4000*4000=16 million $f(\boldsymbol{r})$s must be compared with each other in one geolocating process, which almost impossible for a real-time system.

Fortunately, the Graphics Processing Unit (GPU) parallel computing technique provides a solution to accelerate the GTA process. GPU, which is designed on Single Instruction Multiple Data architecture (SIMD), contains an array of Streamer Multiprocessors (SM). Each SM has a large number of Arithmetic Logic Units (ALUs) with only one control unit. All ALUs in one SM run the same instruction synchronously. The unique configuration of GPU makes it inherently conducive to numerical computing. Taking the lightning geolocation as an example, when applying GPU parallel computing to TOA technique, each ALU will run as one parallel thread to calculate one $f(\boldsymbol{r})$. All threads have the same function to run but with different data streams. Once all $f(\boldsymbol{r})$ s are calculated, a reduction algorithm can be invoked to find the smallest $f(\boldsymbol{r})$ in a parallel manner.

B. CUDA programming model

CUDA is a general-purpose parallel computing platform that utilizes GPU to solve a large-scale parallel problem. CUDA was first introduced by NVIDIA in 2006 [51] and is now widely used in parallel scientific computing scenarios. It provides a high-level model to program GPU-based parallel applications. Below is a briefing of the hierarchy of CUDA. CUDA provides a 3-level hierarchy to configure and invoke threads running on GPU, i.e., GRID, BLOCK and THREAD.

Fig.2 is an illustration of the 3-level hierarchy of the CUDA programming model. As shown in the figure, the GRID consists of BLOCKs, and each BLOCK consists of many THREADs. The dimension of the GRID and BLOCK can be 2 or 3. Once all model arguments are transferred, a kernel function will then be run on all threads with a specified GRID and BLOCK dimensions. In geolocation applications, GRID points are assigned to each THREAD, which has the same kernel function for calculating the $f(\boldsymbol{r})$ as Eq. (2), but with different arguments (i.e., latitude, longitude and altitude at each point).

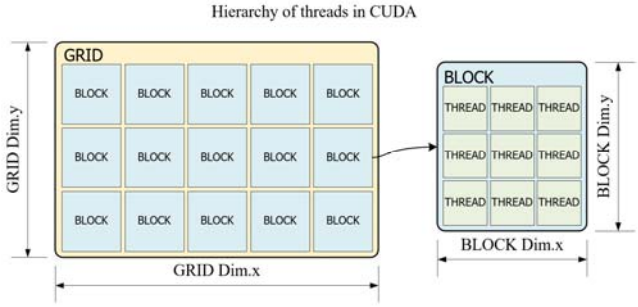

Fig.2 An illustration of the thread hierarchy of CUDA programming model. The GRID consists of a 2 or 3-dimensional matrix of BLOCKs, and each BLOCK consists of parallel THREADs. For specified GRID and BLOCK dimensions and a collective kernel function, the program runs in parallel for all THREADs

C. Optimal parallel reduction algorithm in CUDA

The final step in GTA is to find the point that has the smallest $f(\boldsymbol{r})$. This kind of job can only be run sequentially on a CPU-based platform. Even on a GPU-based parallel architecture, all threads cannot compare their $f(\boldsymbol{r})s$ concurrently. Therefore, a parallel reduction algorithm is necessary for the optimization of this job [52].

Fig.3 is a sketch map illustrating the parallel reduction algorithm. As shown in the figure, the output from every 2 threads in one step are compared and the one with smaller $f(\boldsymbol{r})$ is swapped frontward in each thread. In this way, the smallest one will be quickly converged to the first thread in a few steps. The stride between the 2 competitors in each step is $N/2^i$, where N is the amount of total grid points in a lightning location network and i the index number of the step. As such, the smallest $f(\boldsymbol{r})$ will be quickly shifted to the first thread in a loop index of $log_2 N$, which leads to the final location result. More details of the parallel reduction algorithm can be found in [52].

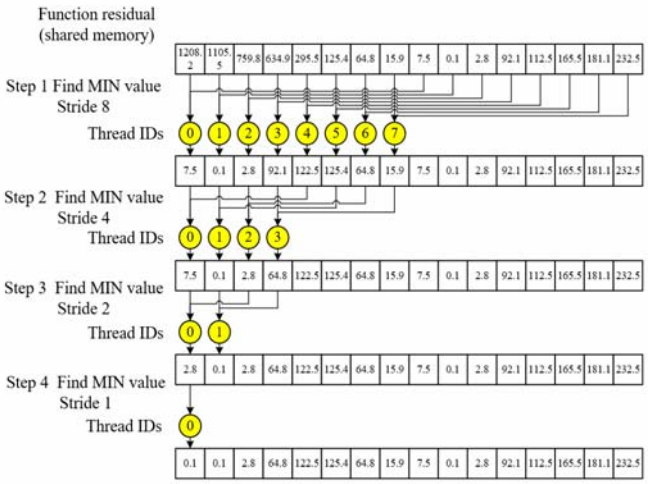

Fig.3 A sketch map of parallel reduction algorithm on picking out the smallest f(r). In a recursive structure, in each step, all threads are divided into two equal groups, each thread in group A compares its *f(r)* with one in group B, transferring the smaller f(r) to group A and discarding the thread in group B. After a thread synchronization, all group A threads then go to the next run until only one residual thread left in group A.

D. GPU-GTA for 3D lightning location

The GPU-GTA algorithm can be easily extended to a 3D lightning location network or any other coordinates that have a describable objective function. For a 3D location, it needs to introduce a new argument – altitude *h*:

$$d(\boldsymbol{r},\boldsymbol{r_i}) = \sqrt{\big(R\big(1-cos(\theta)\big)+h\big)^2 + (Rsin(\theta))^2} \quad (3)$$

Here the Earth curvature is considered. Where θ is the arc length between the two points, R the earth radius or the local radius in an ellipsoidal coordinate and h the altitude.

E. The multi-grid traverse technique

A 3D geolocation domain usually has a large number of grid points. If the grid amount is extremely large, like the traditional GTA, a multi-grid traverse technique can be introduced to further speed up the GPU-GTA process. The multi-grid traverse technique can be applied at least twice in a traverse to find the final solution. It firstly traverses the whole region with a rough grid step to find an initial result and then traverses a small region centered at the initial result with a finer grid to retrieve the final solution.

III. Validation of GPU-GTA with Monte Carlo Simulation for Various Networks

In this section, we validate the GPU-GTA algorithm by implementing Monte Carlo simulations of geolocation errors in different sorts of lightning networks [9]. In the simulation, random time errors are introduced to true arrival times in the geolocation algorithm and possible location error patterns are estimated by comparing the GPU-GTA location results with the true locations. This is the basic idea to understand the accuracy of a lightning location network or test the location algorithm. For doing this, firstly, a Gaussian distributed time error is applied to each true arrival time from each pre-built location point to each sensor in a given lightning location network. Secondly, the 'deviated' arrival times are input into the GPU-GTA or CPU-GTA to calculate the locations with errors. Thirdly, the calculated locations and their pre-built locations are compared to find the location errors (the distance differences between the two sets of locations). Then, the spatial pattern of the location errors in the region covered by the location network is obtained by averaging the location errors from at least 50 times of simulations. Finally, the performance of GPU-GTA and that of CPU-GTA are compared, and thus a benchmark to the GPU-GTA algorithm is given. The initial pre-built location at each point is randomly generated.

A. For a long-baseline 2D lightning location network

To test GPU-GTA in a 2D location case, the network operated by the University of Science and Technology of China is chosen [6, 44]. This network was firstly deployed in 2012 in Anhui province over East China, with an upgrade conducted in 2015, which was named as JASA network since then. The network was specially designed for lower ionosphere remote sensing [53-55], and the GPU-GTA is already running in this network, which yielded good data revealing the association of the Narrow Bipolar Events with and the Blue Jets [56].

JASA consists of 6 sensors as illustrated in **Fig.4**. Its coverage is 1000 km x 1000 km from west to east and from south to north, and the grid searching step for running GPU-GTA is in two level grids with the multi-grid technique. The 1st level grid is 512*512 with a grid step of 2 km. The 2nd level grid is 512*512 with a grid step of 125 m, which is centered at the position estimated from the 1st level grid. In conducting the Monte Carlo simulation of location errors, a 1 μs RMS Gaussian-distributed time error and a linear propagation delay of 100 km per 1 μs (the σ in $f(\boldsymbol{r})$) are introduced to each event arrival time at each sensor.

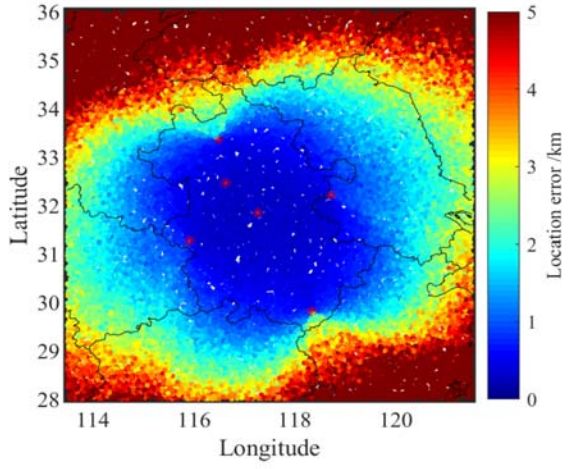

Fig.4 Simulated location error pattern for JASA network running GPU-GTA with Monte Carlo method. The JASA consists of 6 sensors separated over the area of central China, where the red asterisks indicate the 6 sensors. The color of each dot represents the averaged location error at each random location over the network covering region.

The location error pattern at each randomly generated location point is shown in **Fig.4**. As shown by the figure, location errors of GPU-GTA are smaller than 0.5 km inside the inner polygon region of the network, indicating a high performance of GPU-GTA running on JASA in 2D.

B. For a short-baseline 3D lightning mapping array

To test GPU-GTA in a 3D location case, the low-frequency interferometric-TOA lightning mapping array (LFI-LMA) run by Duke University during 2014 is chosen [17]. The LFI-LMA consists of 5 sensors separated by 15 to 20 km, as illustrated in **Fig.5**. This portable network can be easily deployed to image the 3D structure and dynamic development of lightning during thunderstorms [57].

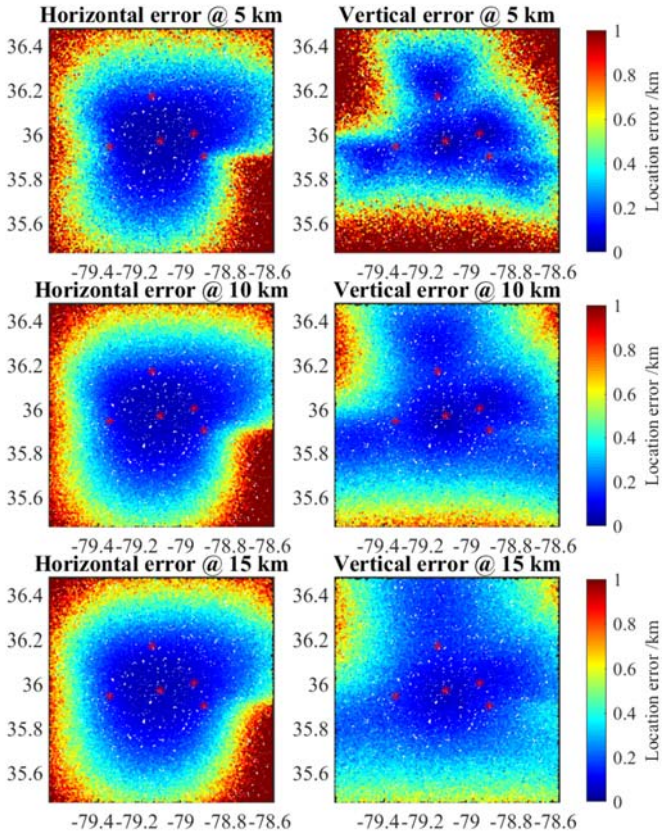

Fig.5 Simulated location error patterns for Duke LFI-LMA network running GPU-GTA algorithm with Monte Carle method. The LFI-LMA was consisted of 5 sensors separated by 15 to 20 km around Duke University, where the red asterisks indicate the 5 sensors' locations. The color of each dot represents the averaged location error at each random location over the network covering region. The top two subplots are for the horizontal (left) and vertical (right) errors for the altitude of 5 km, and the middle two and the bottom two for that of the altitude of 10 km and 15 km, respectively.

Similar to a 2D situation, with a 0.1 μs RMS Gaussian-distributed time error introduced to the true time of arrival, the location error patterns are obtained with the Monte Carlo simulation with GPU-GTA. It is implemented in a 3-level grid approach, the 1st level is 256*256*18 grids with a step of 1 km, the 2nd level is 32*32*16 with a step of 0.4 km, and the 3rd level is 128*128*120 with a step of 25 m. The 2nd level grid is centered at the position estimated from the 1st level one, and the 3rd level grid is centered at the position estimated from the 2nd level one. The results are shown in **Fig.5**, where the horizontal (left) and vertical (right) location errors for the altitude of 5 km, 10 km, and 15 km are shown in subplots from top to bottom in the figure respectively. As shown by the figure, the location error is much smaller at a higher altitude, with the error being less than 200 m over a much larger area at an altitude of 15 km. In a 3D situation, since the solution surface of a baseline close to the ground tends to be tangential to the solution surface of another baseline, this may cause larger vertical uncertainty when close to the ground. The results show that LFI-LMA running GPU-GTA in 3D can perform quite well, with the location errors being less than 200 m over most of the network coverage.

C. Location accuracy of networks running GPU-GTA with different grid steps

The geolocation accuracy is heavily subjected to the grid step used in GPU-GTA. Theoretically, if the grid step is finer enough, GPU-GTA can provide the ultimate location accuracy. However, a real lightning location system always has certain deviations that limit the ultimate location accuracy the system can achieve. One such deviation is the time measuring the uncertainty of sensors in a network. It may come from the GPS timing uncertainty, data acquisition sampling rate, system operating bandwidth, signal-to-noise ratio as well as the method to extract the times from the recorded signals at different sensors. While most of these factors are system hardware-related, we just discuss the location accuracy versus the grid step under a fixed time uncertainty. This is particularly needed for finding the limitation of a network running GPU-GTA.

Fig.6 shows the statistics of 2D location errors in JASA running GPU-GTA with different grid steps, where a time uncertainty of 1 μs RMS is applied. As shown by the figure, considering the total number of points with location errors less than 500 m as a benchmark, it is 4174, 4684 and 4746 for the final grid step of 500 m, 250 m and 125 m respectively. From the grid step of 500 m to 250 m, the number of highly accurate locations increases by 510 or 12%. But from the grid step of 250 m to 125 m, that number only increases by 62 or 1.3%. This property could be attributed to the 1 μs RMS time uncertainty introduced to each sensor, making the network with a location ambiguity between 250 m and 500 m. This suggests that 250 m may be the most economical grid step for JASA running GPU-GTA algorithm with a time uncertainty of 1 μs RMS, resulting in an ultimate location accuracy of about 250 m.

Shown in **Fig.7** is the histogram of 3D location errors of Duke LFI-LMA running GPU-GTA with different grid steps and 0.1 μs RMS time uncertainty at the altitude of 10 km. With the number of location point whose error is less 100 m as a reference, when the grid step decreases from 100 m to 50 m, this number increases from 1675 to 2154, a big increase of 479 or 29%. However, when the grid step further decreases from 50 m to 25m, this number increases from 2154 to 2307, just an increase of 153 or 7%. This suggests that the most economical grid step for LFI-LMA running GPU-GTA algorithm with a time uncertainty of 0.1 μs RMS may be 50 m, resulting in an ultimate location accuracy of about 50 m.

Above results indicate that GPU-GTA can work well with a reasonably high location accuracy in the inner region of either a 2D network like JASA or a 3D network like LFI-LMA. Also, the results show that the location accuracy is limited by the level of the inherent time uncertainty of the network, rather than the grid step if the grid step is small enough. GPU-GTA can give the ultimate accurate result when the grid step is suitable.

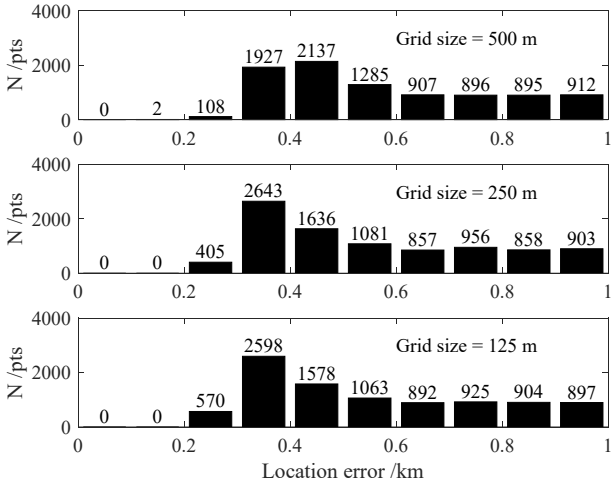

Fig.6 Statistics of 2D location errors in first 1 km of JASA running GPU-GTA with different grid steps and 1us RMS time uncertainty. The subplots from top to bottom are for the grid step of 500 m, 250 m and 125 m respectively.

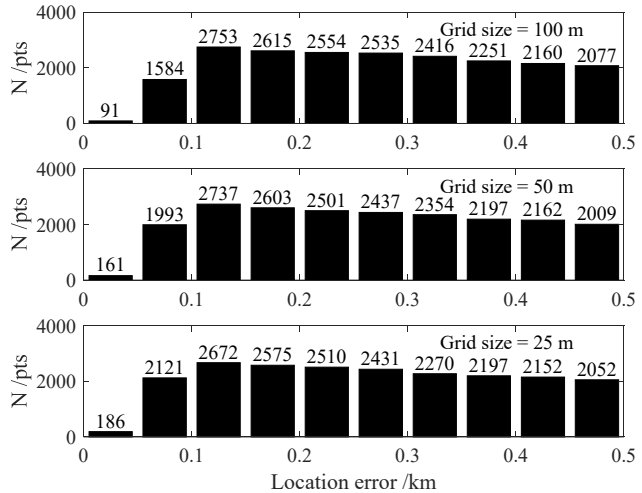

Fig.7 Statistics of 3D location errors in first 500 m of Duke LFI-LMA running GPU-GTA with different grid steps and 0.1 us RMS time uncertainty at the altitude of 10 km. The subplots from top to bottom are for the grid step of 100 m, 50 m and 25 m respectively.

IV. Performance of GPU-GTA

The most significant merit of GPU-GTA algorithm is that it

can greatly increase the speed of computation compared to CPU-GTA. The processing speed is crucial to a lightning location network, especially for those built for real-time reporting. To have a quantitative evaluation of the GPU-GTA performance, we estimate the processing time for locating a certain number of events under a specific network with GPU-GTA and compare it to that of CPU-GTA.

Fig.8 is a comparison of the processing times between the CPU-GTA and GPU-GTA for locating 100 to 1000 lightning events in a 3-sensor 2D network with a grid extension of 2000*2000. Under such a configuration, locating one lightning event needs the GTA algorithm traversing all the 4 million points. As can be seen from the figure, the GPU-GTA is generally 2700 times faster than the CPU-GTA under such a configuration.

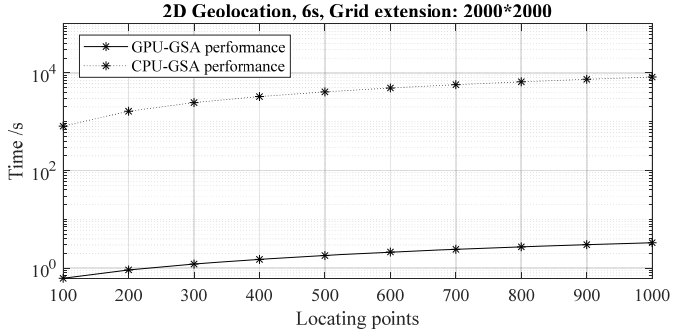

Fig.8 A comparison of the processing time between the CPU-GTA and GPU-GTA for locating 100 to 1000 events in a 3-sensor 2D network with a grid extension of 2000*2000. Dot-line is for CPU-GTA and solid-line is for GPU-GTA.

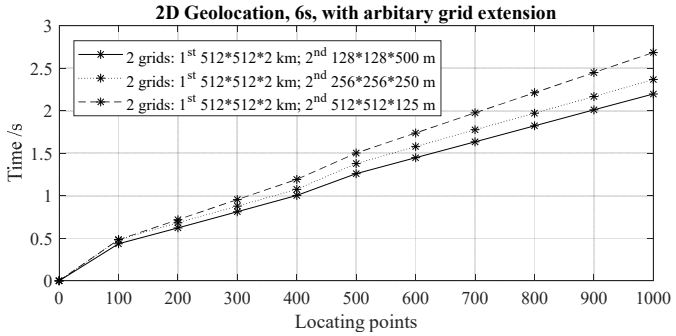

Fig.9 Comparisons of processing times of GPU-GTA operated in a 6-sensor 2D network like JASA with 3 different sets of grid steps and extensions. While the 1st level grid is set with a grid step and an extension of 2 km and 512*512, the 2nd level grid is set with three diferent grid steps / extensions of 500 m/128*128 (solid-line), 250 m / 256*256 (dot-line), and 125 m / 512*512 (dash-line), respectively.

Fig.9 is a comparison of the computing speeds of the GPU-GTA between 3 different setups of a two-level-grid traverse technique for a 6-sensor 2D network like JASA. In a two-level-grid traverse technique, the traversing process can start with a relatively big initial grid step (e.g., 2 km). Once an initial event position is acquired with the initial grid step, a finer grid step (e.g., 125 m) can be taken to traverse a small space centered at the initial position to get the accurate event position. In the figure, while the 1st level grid is set at a step of 2 km with an extension of 512*512, the 2nd level grid is set at three different steps of 500 m, 250 m and 125 m corresponding to three different extensions of 128*128, 256*256 and 512*512, respectively.

As can be seen from the figure, with the increase of the grid extension, the processing time increases linearly. It costs about 2.7 seconds to locate 1000 events in this 6-sensor network covering an area of 1000 km x 1000 km with the grid step of 125 m. Such a computing speed could be efficient enough for a real-time lightning network.

Similar to the 2D case, the performance of GPU-GTA in a 3D network is also evaluated.

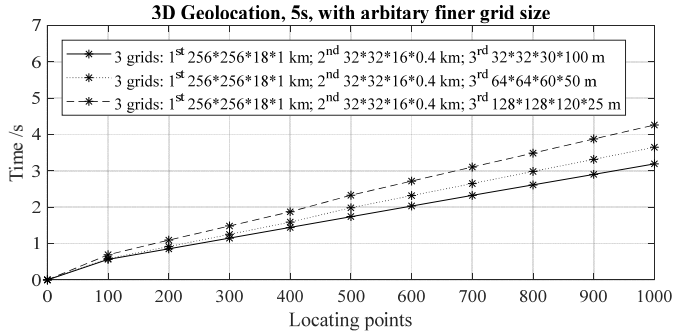

Fig.10 Comparisons of processing times of GPU-GTA running in a 5-sensor 3D network like LFI-LMA with a three-level-grid traverse technique under 3 different grid step and extension settings. The 1st and 2nd level grid steps are 1 km and 0.4 km with a grid extension of 256*256*18 and 32*32*16, respectively. The 3rd level (final) grid is set with three diferent steps / extensinos of 100 m / 32*32*30, (solid-line), 50 m / 64*64*60 (dot-line) and 25 m / 128*128*120 (dashed-line), respectively.

Fig.10 shows the processing times of GPU-GTA operated in a 5-sensor 3D network like LFI-LMA with a three-level-grid traverse technique with 3 different grid settings. The 1st level (initial) grid is set with a step of 1000 m and an extension of 120*120*18, corresponding to a cube of 256 km*256 km*18 km (altitude). The 2nd level grid is set with a step of 0.4 km and an extension of 32*32*16. The 3rd level (final) grid is set with three different grid steps of 100 m, 50 m and 25 m respectively with a grid extension of 32*32*30, 64*64*60 and 128*128*120 respectively, corresponding to a cube of 3.2 km*3.2 km*3.2 km centered at the position estimated from the 2nd level grid. As shown by the figure, it takes about 3.2 seconds, 3.6 seconds and 4.3 seconds to locate 1000 points in 3D at the accuracy of 100 m, 50 m and 25 m respectively. Again, the speed of GPU-GTA is efficient enough to satisfy a real-time 3D lightning network like LFI-LMA. It should be pointed out that the computing platform for the CPU- and GPU-based GTA in this study are Core i7 6700k and GeForce GTX 1080ti respectively. The GPU-GTA algorithm should be much faster on a better GPU workstation.

V. Conclusion

A GPU-based grid traverse geolocation algorithm (GPU-GTA) for lightning location networks is proposed and examined. The overall performance of GPU-GTA is examined by applying it to JASA (a 6-sensor 2D lightning location network in central China) and LFI-LMA (a 5-sensor 3D lightning mapping array in Duke University). The results show that the GPU-GTA algorithm can be easily implemented in both 2D and 3D lightning geolocation networks or any other multi-station networks. The location accuracy of GPU-GTA is

validated with Monte Carol simulations. The results show that GPU-GTA can locate a lightning source with sufficient accuracy over the coverage of a network. The processing time of GPU-GTA to locate a lightning event is found to be 2700 times faster than that of CPU-GTA, making GPU-GTA efficient enough for locating a source in 3D in real-time.

Moreover, GPU-GTA can give a more accurate lightning event location than the traditional one. As we know, most existing lightning location networks are based on real-time analytical solutions of certain simple models, while the reality is much more complicated. With GPU-GTA, for a given network, one can build up a database based on numerical solutions of certain complete models under various scenarios in advance, the lightning event location can then be easily determined with the grid traverse algorithm in real-time. For example, the Earth ground is rough, and its topography always causes inherent propagation delay of the lightning electromagnetic pulse to sensors away from the lightning source. This kind of time delay can be easily predicted with FDTD wave simulation in advance and pre-input to the GTA database [47]. GPU-GTA can then take this pre-input time delay into account to get a more accurate lightning event location than the traditional one.

REFERENCES

[1] X.-M. Shao, M. Stanley, A. Regan, J. Harlin, M. Pongratz, and M. Stock, "Total Lightning Observations with the New and Improved Los Alamos Sferic Array (LASA)," *Journal of Atmospheric & Oceanic Technology,* vol. 23, no. 10, 2006.

[2] D. Smith *et al.*, "The Los Alamos Sferic Array: A research tool for lightning investigations," *Journal of Geophysical Research: Atmospheres (1984–2012),* vol. 107, no. D13, pp. ACL 5-1-ACL 5-14, 2002.

[3] K. L. Cummins and M. J. Murphy, "An overview of lightning locating systems: History, techniques, and data uses, with an in-depth look at the US NLDN," *Electromagnetic Compatibility, IEEE Transactions on,* vol. 51, no. 3, pp. 499-518, 2009.

[4] Y. Wang *et al.*, "Beijing Lightning Network (BLNET) and the observation on preliminary breakdown processes," *Atmospheric Research,* vol. 171, pp. 121-132, 2016.

[5] C. Rodger *et al.*, "Detection efficiency of the VLF World-Wide Lightning Location Network (WWLLN): initial case study," in *Annales Geophysicae*, 2006, vol. 24, no. 12, pp. 3197-3214.

[6] Z. Qin, B. Zhu, F. Lyu, M. Ma, and D. Ma, "Using time domain waveforms of return strokes to retrieve the daytime fluctuation of ionospheric D layer(in Chinese)," *Chinese Science Bulletin,* no. 7, pp. 654-663, 2015.

[7] H. D. Betz *et al.*, "LINET—an international lightning detection network in Europe," *Atmospheric Research,* vol. 91, no. 2, pp. 564-573, 2009.

[8] J. Montanyà, N. Pineda, V. March, A. Illa, D. Romero, and G. Solà, "Experimental evaluation of the Catalan lightning detection network," in *19th International Lightning Detection Conference, Tucson*, 2006.

[9] W. Koshak *et al.*, "North Alabama Lightning Mapping Array (LMA): VHF source retrieval algorithm and error analyses," *Journal of Atmospheric and Oceanic Technology,* vol. 21, no. 4, pp. 543-558, 2004.

[10] C. A. Morales *et al.*, "years of Sferics Timing And Ranging NETwork–STARNET: A lightning climatology over South America," in *23rd International Lightning Detection Conference & 5th International Lightning Meteorology Conference*, 2014, pp. 271-350.

[11] R. Said and M. Murphy, "GLD360 upgrade: Performance analysis and applications," in *24th International Lightning Detection Conference*, 2016: CA San Diego.

[12] C. Liu and S. Heckman, "Using total lightning data in severe storm prediction: global case study analysis from North America, Brazil and Australia," in *2011 International Symposium on Lightning Protection*, 2011: IEEE, pp. 20-24.

[13] K. L. Cummins, M. J. Murphy, E. A. Bardo, W. L. Hiscox, R. B. Pyle, and A. E. Pifer, "A combined TOA/MDF technology upgrade of the US National Lightning Detection Network," *Journal of Geophysical Research: Atmospheres,* vol. 103, no. D8, pp. 9035-9044, 1998.

[14] S. J. Keogh, E. Hibbett, J. Nash, and J. Eyre, "The Met Office Arrival Time Difference (ATD) system for thunderstorm detection and lightning location," *Met Office Forecasting Research Tech. Rep,* vol. 488, p. 22, 2006.

[15] K. Lagouvardos, V. Kotroni, H.-D. Betz, and K. Schmidt, "A comparison of lightning data provided by ZEUS and LINET networks over Western Europe," *Natural Hazards Earth System Sciences,* vol. 9, no. 5, pp. 1713-1717, 2009.

[16] Z. Qin, B. Zhu, M. Chen, M. Ma, and D. Ma, "Configuration of a VLF/LF Lightning Detection Network in Central China and Its application," presented at the 2015 9th Asia-Pacific International Conference on Lightning (APL2015), 2015.

[17] F. Lyu *et al.*, "A low-frequency near-field interferometric-TOA 3-D Lightning Mapping Array," *Geophysical Research Letters,* 2014.

[18] D. Shi *et al.*, "Low-frequency E-field Detection Array (LFEDA)—Construction and preliminary results," *Science China Earth Sciences,* vol. 60, no. 10, pp. 1896-1908, 2017.

[19] W. Rison, R. J. Thomas, P. R. Krehbiel, T. Hamlin, and J. Harlin, "A GPS - based three - dimensional lightning mapping system: Initial observations in central New Mexico," *Geophysical Research Letters,* vol. 26, no. 23, pp. 3573-3576, 1999.

[20] P. M. Bitzer *et al.*, "Characterization and applications of VLF/LF source locations from lightning using the Huntsville Alabama Marx Meter Array," vol. 118, no. 8, pp. 3120-3138, 2013.

[21] T. Wu, D. Wang, and N. J. G. R. L. Takagi, "Lightning mapping with an array of fast antennas," vol. 45, no. 8, pp. 3698-3705, 2018.

[22] D. E. Proctor, "A hyperbolic system for obtaining VHF radio pictures of lightning," *Journal of Geophysical Research,* vol. 76, no. 6, pp. 1478-1489, 1971.

[23] D. Boccippio, S. Heckman, and S. Goodman, "A diagnostic analysis of the Kennedy Space Center LDAR network: 1. Data characteristics," *Journal of Geophysical Research: Atmospheres,* vol. 106, no. D5, pp. 4769-4786, 2001.

[24] D. Boccippio, S. Heckman, and S. Goodman, "A diagnostic analysis of the Kennedy Space Center LDAR network: 2. Cross-sensor studies," *Journal of Geophysical Research: Atmospheres,* vol. 106, no. D5, pp. 4787-4796, 2001.

[25] R. J. Thomas *et al.*, "Accuracy of the lightning mapping array," *Journal of Geophysical Research: Atmospheres,* vol. 109, no. D14, 2004.

[26] M. Qing, Z. Yijun, and H. Ping, "Lightning observation and field experiment with 3D SAFIR system during summer 2003 in Beijing-Hebei Area," *27th Int. Conf. Lightning Protection,* vol. 4, pp. 101-104, 2005.

[27] E. Defer *et al.*, "Lightning activity for the July 10, 1996, storm during the Stratosphere - Troposphere Experiment: Radiation, Aerosol, and Ozone-A (STERAO-A) experiment," *Journal of Geophysical Research: Atmospheres,* vol. 106, no. D10, pp. 10151-10172, 2001.

[28] P. Richard, A. Soulage, P. Laroche, and J. Appel, "The SAFIR lightning monitoring and warning system, applications to aerospace activities," in *Lightning and Static Electricity*, 1988.

[29] W. J. Koshak and R. Solakiewicz, "TOA lightning location retrieval on spherical and oblate spheroidal earth geometries," *Journal of Atmospheric and Oceanic Technology,* vol. 18, no. 2, pp. 187-199, 2001.

[30] E. P. Krider, R. C. Noggle, and M. A. Uman, "A gated, wideband magnetic direction finder for lightning return strokes," *Journal of Applied Meteorology,* vol. 15, no. 3, pp. 301-306, 1976.

[31] K. L. Cummins and M. J. Murphy, "An overview of lightning locating systems: History, techniques, and data uses, with an in-depth look at the US NLDN," *IEEE Transactions on Electromagnetic Compatibility,* vol. 51, no. 3, pp. 499-518, 2009.

[32] R. L. Dowden, J. B. Brundell, and C. Rodger, "VLF lightning location by time of group arrival (TOGA) at multiple sites," *Journal of Atmospheric Solar-Terrestrial Physics,* vol. 64, no. 7, pp. 817-830, 2002.

[33] M. Akita, M. Stock, Z. Kawasaki, P. Krehbiel, W. Rison, and M. Stanley, "Data processing procedure using distribution of slopes of phase differences for broadband VHF interferometer," *Journal of Geophysical Research: Atmospheres,* 2014.

[34] Z. Sun, X. Qie, M. Liu, D. Cao, and D. Wang, "Lightning VHF radiation location system based on short-baseline TDOA technique—Validation

in rocket-triggered lightning," *Atmospheric Research,* vol. 129, pp. 58-66, 2013.

[35] X.-M. Shao, P. Krehbiel, R. Thomas, and W. Rison, "Radio interferometric observations of cloud-to-ground lightning phenomena in Florida," *Journal of Geophysical Research: Atmospheres (1984–2012),* vol. 100, no. D2, pp. 2749-2783, 1995.

[36] X.-M. Shao, D. Holden, and C. Rhodes, "Broad band radio interferometry for lightning observations," *Geophysical research letters,* vol. 23, no. 15, pp. 1917-1920, 1996.

[37] Z. Kawasaki, R. Mardiana, and T. Ushio, "Broadband and narrowband RF interferometers for lightning observations," *Geophysical research letters,* vol. 27, no. 19, pp. 3189-3192, 2000.

[38] R. Mardiana and Z. Kawasaki, "Broadband radio interferometer utilizing a sequential triggering technique for locating fast-moving electromagnetic sources emitted from lightning," *Instrumentation and Measurement, IEEE Transactions on,* vol. 49, no. 2, pp. 376-381, 2000.

[39] C. Rhodes, X. Shao, P. Krehbiel, R. Thomas, and C. Hayenga, "Observations of lightning phenomena using radio interferometry," *Journal of Geophysical Research: Atmospheres,* vol. 99, no. D6, pp. 13059-13082, 1994.

[40] M. Stock *et al.*, "Continuous broadband digital interferometry of lightning using a generalized cross-correlation algorithm," *Journal of Geophysical Research: Atmospheres,* vol. 119, no. 6, pp. 3134-3165, 2014.

[41] J.-Y. Lojou, M. J. Murphy, R. L. Holle, and N. W. Demetriades, "Nowcasting of thunderstorms using VHF measurements," in *Lightning: principles, instruments and applications*: Springer, 2009, pp. 253-270.

[42] C. O. Hayenga and J. W. Warwick, "Two-dimensional interferometric positions of VHF lightning sources," *Journal of Geophysical Research: Oceans (1978–2012),* vol. 86, no. C8, pp. 7451-7462, 1981.

[43] F. Lyu, S. A. Cummer, Z. Qin, and M. Chen, "Lightning initiation processes imaged with very high frequency broadband interferometry," vol. 0, no. ja, 2019.

[44] Z. Qin, "The Observation of Ionospheric D-layer based on the Multi-station Lightning Detection System (in Chinese)," Dissertation of Master Degree, Earth and Space Science, University of Science and Technology of China, Hefei, 2014.

[45] N. Honma, K. L. Cummins, M. J. Murphy, A. E. Pifer, T. J. I. T. o. P. Rogers, and Energy, "Improved lightning locations in the Tohoku Region of Japan using propagation and waveform onset corrections," vol. 133, no. 2, pp. 195-202, 2013.

[46] W. Schulz, G. Diendorfer, S. Pedeboy, D. R. J. N. H. Poelman, and E. S. Sciences, "The European lightning location system EUCLID–Part 1: Performance analysis and validation," vol. 16, no. 2, pp. 595-605, 2016.

[47] T. Lu and M. Chen, "Modelling of effect of propagation of lightning electromagnetic pulse over rough ground," in *Electromagnetic Compatibility (APEMC), 2016 Asia-Pacific International Symposium on*, 2016, vol. 1: IEEE, pp. 155-157.

[48] D. Li *et al.*, "On lightning electromagnetic field propagation along an irregular terrain," vol. 58, no. 1, pp. 161-171, 2016.

[49] D. Li, M. Rubinstein, F. Rachidi, G. Diendorfer, W. Schulz, and G. J. J. o. G. R. A. Lu, "Location accuracy evaluation of ToA-based lightning location systems over mountainous terrain," vol. 122, no. 21, 2017.

[50] C. Nvidia, "Programming guide," ed, 2010.

[51] C. Nvidia, "Compute unified device architecture programming guide," 2007.

[52] M. Harris, "Optimizing parallel reduction in CUDA," *NVIDIA Developer Technology,* vol. 2, p. 45, 2007.

[53] F. Liu, Z. Qin, B. Zhu, M. Ma, M. Chen, and P. Shen, "Observations of ionospheric D layer fluctuations during sunrise and sunset by using time domain waveforms of lightning narrow bipolar events," (in Chinese), *Chinese Journal of Geophysics-Chinese Edition,* vol. 61, no. 2, pp. 484-493, Feb 2018.

[54] Z. Qin, M. Chen, B. Zhu, and Y. p. Du, "An improved ray theory and transfer matrix method-based model for lightning electromagnetic pulses propagating in Earth-ionosphere waveguide and its applications," *Journal of Geophysical Research: Atmospheres,* 2017.

[55] Z. Qin, M. Chen, and B. Zhu, "Study of earth-ionosphere waveguide effect on lightning pulse with Ray Theory," in *Lightning Protection (ICLP), 2016 33rd International Conference on*, 2016: IEEE, pp. 1-5.

[56] F. Liu *et al.*, "Observations of Blue Discharges Associated With Negative Narrow Bipolar Events in Active Deep Convection," (in English), *Geophysical Research Letters,* vol. 45, no. 6, pp. 2842-2851, Mar 28 2018.

[57] F. Lyu, S. A. Cummer, G. Lu, X. Zhou, and J. Weinert, "Imaging lightning intracloud initial stepped leaders by low-frequency interferometric lightning mapping array," *Geophysical Research Letters,* vol. 43, no. 10, pp. 5516-5523, 2016.